**Developmental Cell, Volume *48***

## Supplemental Information

# Adhesive L1CAM-Robo Signaling Aligns Growth Cone F-Actin Dynamics to Promote Axon-Dendrite Fasciculation in *C. elegans*

**Chun-Hao Chen, Hao-Wei Hsu, Yun-Hsuan Chang, and Chun-Liang Pan**

**SUPPLEMENTAL INFORMATION**

Supplemental Figures 1-6

Supplemental Figure Legends

Supplemental Movies 1-6

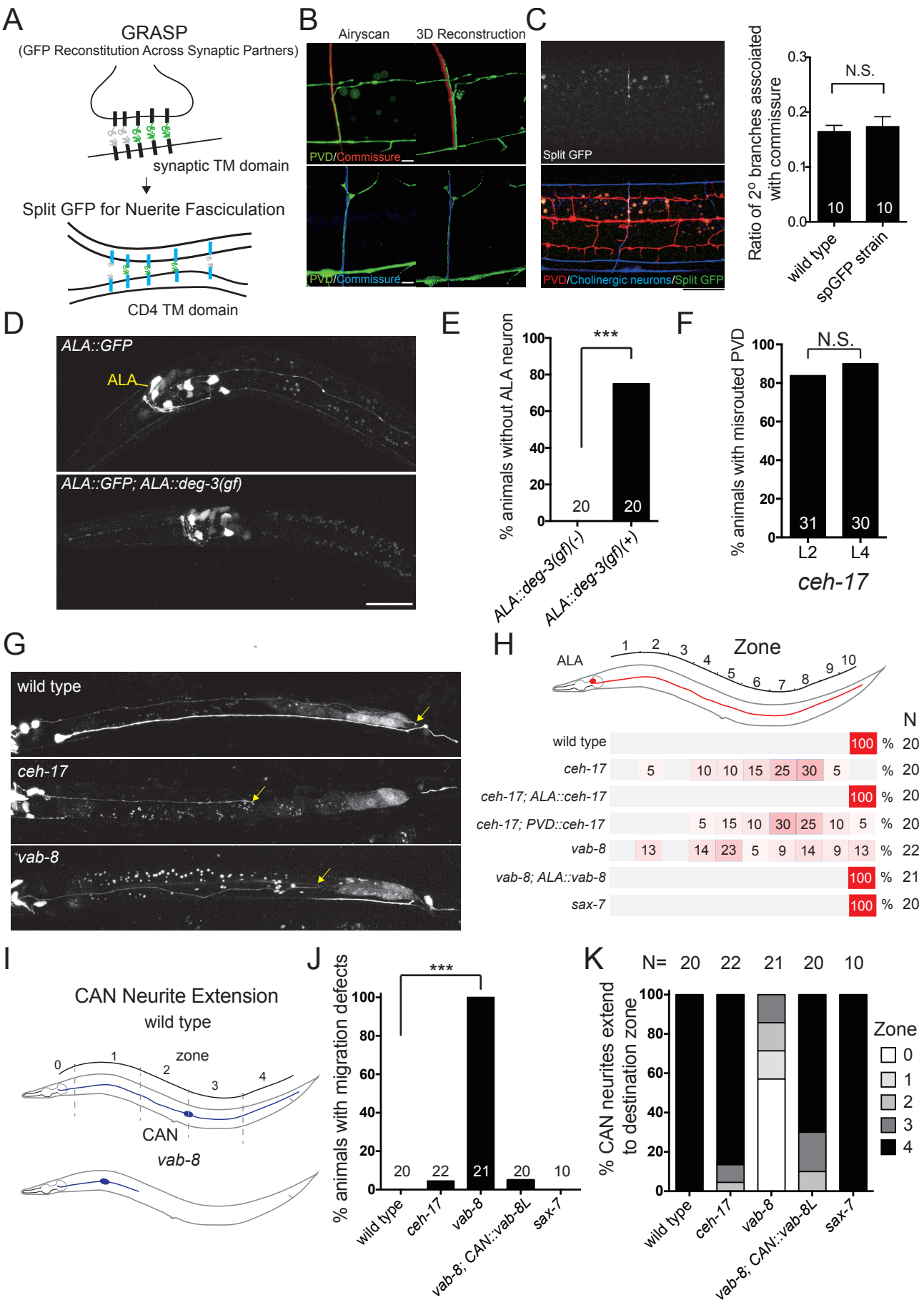
A
GRASP
(GFP Reconstitution Across Synaptic Partners)
synaptic TM domain
Split GFP for Nuerite Fasciculation
CD4 TM domain
B
Airyscan
3D Reconstruction
PVD/Commissure
PVD/Commissure
C
Split GFP
PVD/Cholinergic neurons/Split GFP
Ratio of 2° branches asscoiated with commissure
N.S.
10
10
wild type
spGFP strain
D
ALA::GFP
ALA
ALA::GFP; ALA::deg-3(gf)
E
% animals without ALA neuron
***
20
20
ALA::deg-3(gf)(-)
ALA::deg-3(gf)(+)
F
% animals with misrouted PVD
N.S.
31
30
L2
L4
ceh-17
G
wild type
ceh-17
vab-8
H
ALA
Zone
N
wild type 100 % 20
ceh-17 5 10 10 15 25 30 5 % 20
ceh-17; ALA::ceh-17 100 % 20
ceh-17; PVD::ceh-17 5 15 10 30 25 10 5 % 20
vab-8 13 14 23 5 9 14 9 13 % 22
vab-8; ALA::vab-8 100 % 21
sax-7 100 % 20
I
CAN Neurite Extension
wild type
zone
CAN
vab-8
J
% animals with migration defects
***
20
22
21
20
10
wild type
ceh-17
vab-8
vab-8; CAN::vab-8L
sax-7
K
N= 20 22 21 20 10
% CAN neurites extend to destination zone
Zone
wild type
ceh-17
vab-8
vab-8; CAN::vab-8L
sax-7

**Figure S1. Development of PVD, ALA and CAN Neurons. Related to Figure 1.**

(A) Schematic diagram of GRASP and split GFP for assaying synaptic connection and neurite fasciculation, respectively. (B) Airyscan projection images (left) and 3D reconstruction (right) of fasciculation between PVD secondary branches and the motor commissures. Red, GABAergic neurons; Blue, Cholinergic neurons. Scale bar = 2 μm. (C) Confocal projection images (left) and quantification (right) of fasciculation between PVD dendrites and cholinergic motor commissures with or without the split GFP transgene. Error bars are S.E.M. N.S., not significant, Student *t* test. (D) Confocal projection images of *ynIs66(Pflp-7::GFP)* with or without expression of *deg-3(gf)* from the ALA (*flp-7*) promoter. Scale bar = 20 μm. (E) Killing efficiency of ALA neurons by *deg-3(gf)* expression. (F) Quantification of misrouted PVD primary dendrites in the *ceh-17* mutant at L2 and L4 stages. (G) Confocal projection images of ALA axon. Anterior is to the left and dorsal side up. Arrows, ends of the ALA axon. (H) Schematic diagram (top) and quantification (bottom) of ALA axon extension (top). Numbers in the diagram are specific anterior-posterior positions along the worm body. Percentage of ALA axon ending at indicated positions are shown. N = animals scored. (I) Schematic diagram of CAN neuron morphology in the wild type and the *vab-8* mutant. Numbers in the diagram are specific anterior-posterior zones along the worm body. (J) Quantification of CAN migration defects. (K) Quantification of CAN extension to indicated body zones. N = animals scored (C, E, F, H, J and K). For (E and J), ***, $p < 0.005$, N.S., not significant, two-proportion z test.

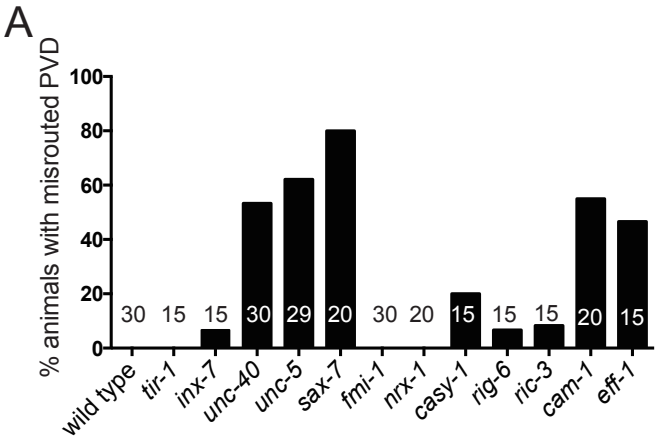
A
% animals with misrouted PVD
100
80
60
40
20
0
30
15
15
30
29
20
30
20
15
15
15
20
15
wild type
tir-1
inx-7
unc-40
unc-5
sax-7
fmi-1
nrx-1
casy-1
rig-6
ric-3
cam-1
eff-1

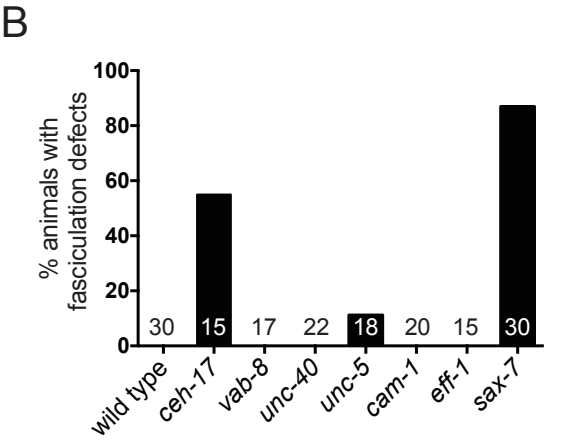
B
% animals with fasciculation defects
100
80
60
40
20
0
30
15
17
22
18
20
15
30
wild type
ceh-17
vab-8
unc-40
unc-5
cam-1
eff-1
sax-7

**Figure S2. A Screen for Candidate Molecules Involved in ALA-PVD Fasciculation. Related to Figure 2.**

(A and B) Quantification of misrouted PVD primary dendrite (A) and ALA-PVD fasciculation defects (B). N = animals scored.

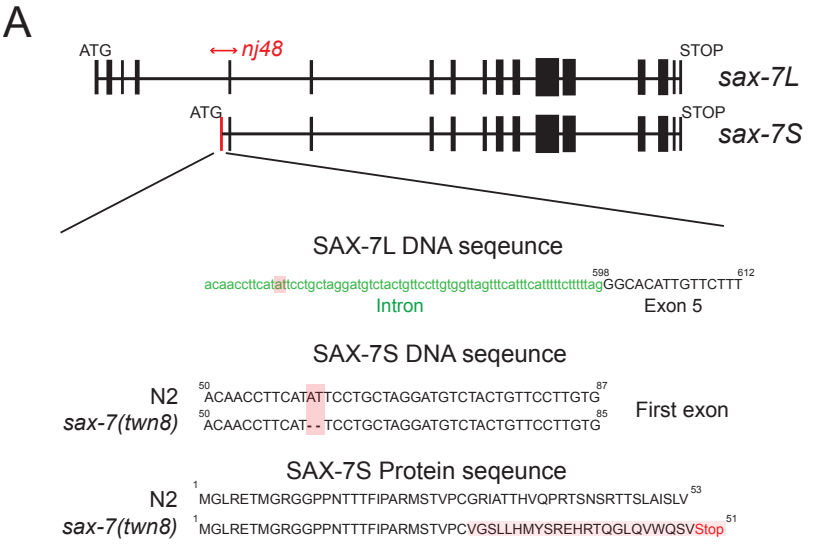
A
ATG
nj48
STOP
sax-7L
ATG
STOP
sax-7S
SAX-7L DNA seqeunce
acaaccttcatattcctgctaggatgtctactgttccttgtggttagtttcatttcatttttcttttagGGCACATTGTTCTTT
598
612
Intron
Exon 5
SAX-7S DNA seqeunce
N2
50
ACAACCTTCATATTCCTGCTAGGATGTCTACTGTTCCTTGTG
87
sax-7(twn8)
50
ACAACCTTCAT--TCCTGCTAGGATGTCTACTGTTCCTTGTG
85
First exon
SAX-7S Protein seqeunce
N2
1
MGLRETMGRGGPPNTTTFIPARMSTVPCGRIATTHVQPRTSNSRTTSLAISLV
53
sax-7(twn8)
1
MGLRETMGRGGPPNTTTFIPARMSTVPCVGSLLHMYSREHRTQGLQVWQSVStop
51

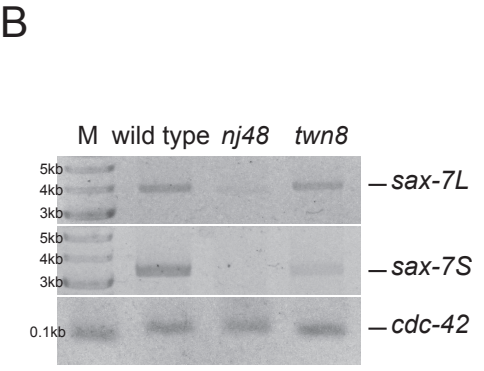
B
M
wild type
nj48
twn8
5kb
4kb
3kb
sax-7L
5kb
4kb
3kb
sax-7S
0.1kb
cdc-42

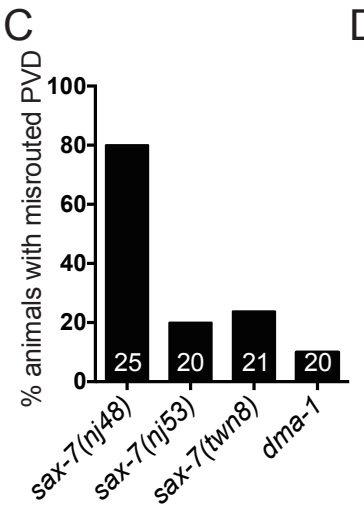
C
% animals with misrouted PVD
100
80
60
40
20
0
25
20
21
20
sax-7(nj48)
sax-7(nj53)
sax-7(twn8)
dma-1

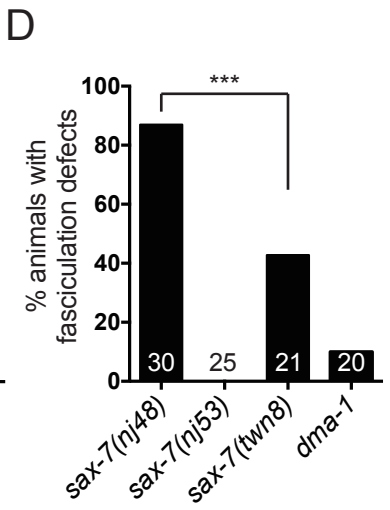
D
% animals with fasciculation defects
***
100
80
60
40
20
0
30
25
21
20
sax-7(nj48)
sax-7(nj53)
sax-7(twn8)
dma-1

**Figure S3. The Role of Different SAX-7 Isoforms in ALA-PVD Fasciculation. Related to Figure 2.**

(A) Generation of the *sax-7S*-specific mutation, *twn8*, by CRISPR-Cas9. Boxes are exons and lines represent introns of the *sax-7* locus. Predicted transcripts of *sax-7S* and *sax-7L* are shown. (B) Reverse transcription (RT)-PCR of *sax-7L* and *sax-7S* transcripts in indicated genotypes. *cdc-42* is used as the internal control. (C and D) Quantification of misrouting of PVD primary dendrites. N = animals scored. ***, $p <$ 0.005, two proportion z test.

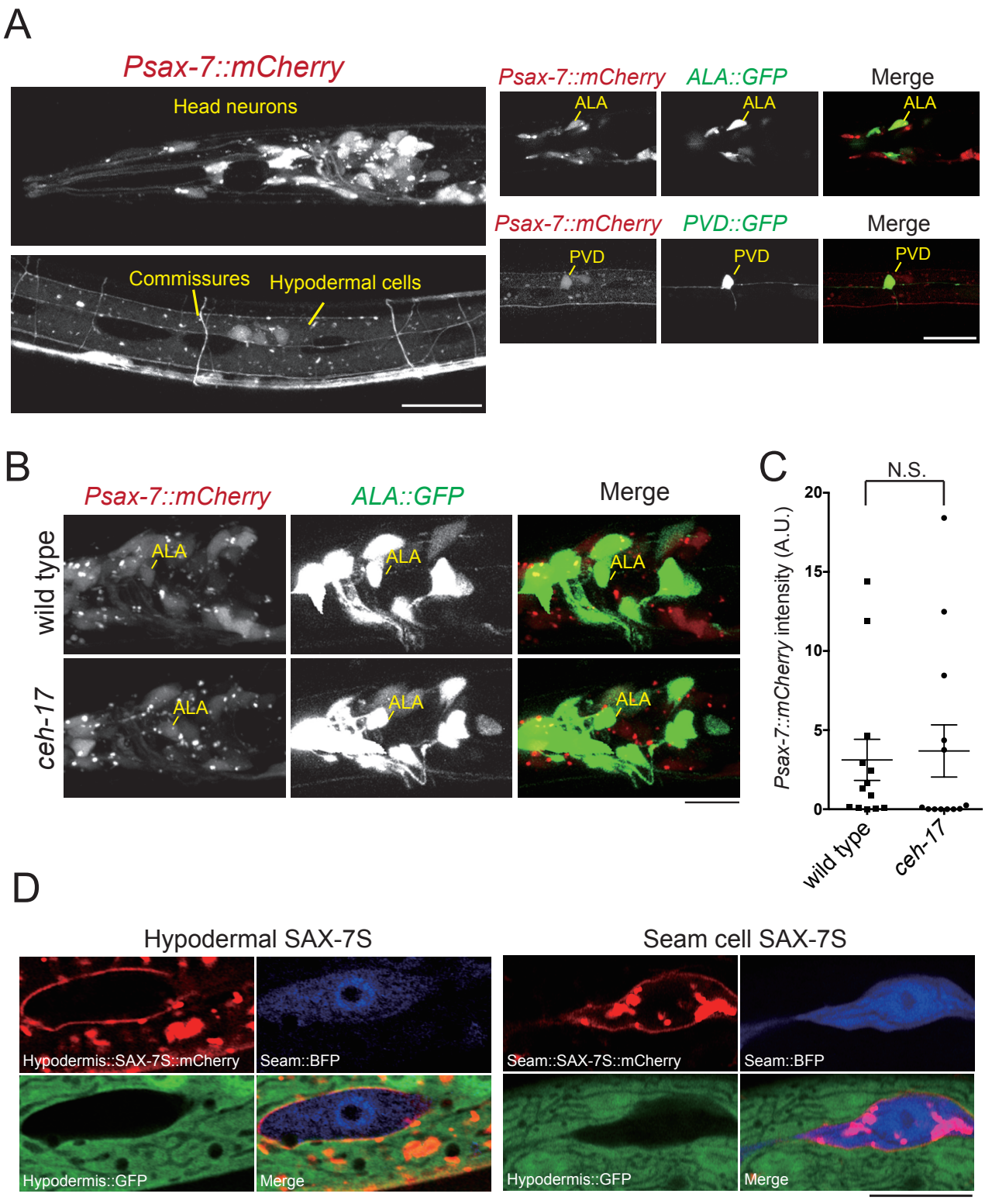
A
Psax-7::mCherry
Head neurons
Commissures
Hypodermal cells
Psax-7::mCherry
ALA::GFP
Merge
ALA
Psax-7::mCherry
PVD::GFP
Merge
PVD
B
Psax-7::mCherry
ALA::GFP
Merge
wild type
ceh-17
ALA
C
N.S.
Psax-7::mCherry intensity (A.U.)
20
15
10
5
0
wild type
ceh-17
D
Hypodermal SAX-7S
Seam cell SAX-7S
Hypodermis::SAX-7S::mCherry
Seam::BFP
Hypodermis::GFP
Merge
Seam::SAX-7S::mCherry
Seam::BFP
Hypodermis::GFP
Merge

**Figure S4. The Expression Pattern of *sax-7*. Related to Figure 2.**

(A) *sax-7* expression pattern revealed by mCherry driven from the 6 kb 5' upstream sequence of *sax-7*. Scale bar = 20 μm. (B) Representative confocal projection images of *Psax-7::mCherry* expression in indicated genotypes. Scale bar = 20 μm. (C) Quantification of *Psax-7::mCherry* signal intensity in ALA. Each dot represents measurement in a single ALA neuron. Error bars are S.E.M. N.S., not significant, Student *t* test. (D) Airyscan projection images of SAX-7S::mCherry driven by hypodermal *dpy-7* and seam cell *scm3* promoters, respectively. Scale bar = 10 μm.

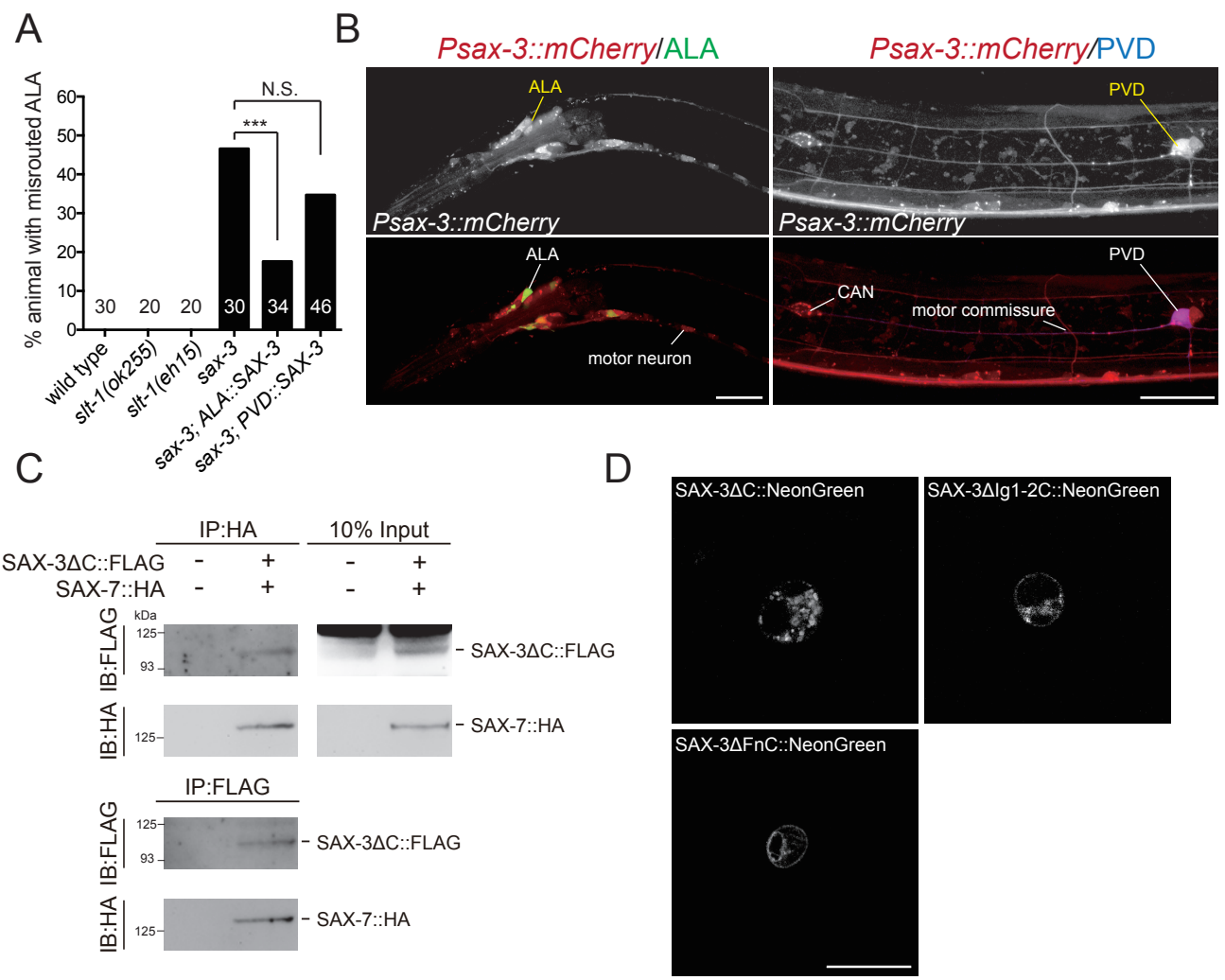
A
% animal with misrouted ALA
60
50
40
30
20
10
0
N.S.
***
30
20
20
30
34
46
wild type
slt-1(ok255)
slt-1(eh15)
sax-3
sax-3; ALA::SAX-3
sax-3; PVD::SAX-3
B
Psax-3::mCherry/ALA
Psax-3::mCherry/PVD
ALA
PVD
Psax-3::mCherry
Psax-3::mCherry
ALA
motor neuron
PVD
CAN
motor commissure
C
IP:HA
10% Input
SAX-3ΔC::FLAG - + - +
SAX-7::HA - + - +
kDa
IB:FLAG
125
93
SAX-3ΔC::FLAG
IB:HA
125
SAX-7::HA
IP:FLAG
IB:FLAG
125
93
SAX-3ΔC::FLAG
IB:HA
125
SAX-7::HA
D
SAX-3ΔC::NeonGreen
SAX-3ΔIg1-2C::NeonGreen
SAX-3ΔFnC::NeonGreen

**Figure S5. The Expression Pattern of *sax-3*, ALA Phenotypes in the *sax-3* Mutant and Coimmunoprecipitation of SAX-7-SAX-3 complex. Related to Figure 3.**

(A) Quantification of misrouted ALA axons. N = animals scored. ***, $p < 0.005$, N.S., not significant, two-proportion z test. (B) *sax-3* expression pattern revealed by the mCherry driven from the 4 kb 5' upstream sequence of *sax-3*. (C) Reciprocal coimmunoprecipitation of FLAG-tagged SAX-3ΔC and HA-tagged SAX-7 expressed in S2 cells. Anti-FLAG band intensity is normalized to that of SAX-3(ΔC) (right). Error bars are S.E.M. **, $p = 0.0065$, Student's t-test. (D) Single confocal optical sections of S2 cells expressing SAX-3 variants. Scale bar = 20 μm.

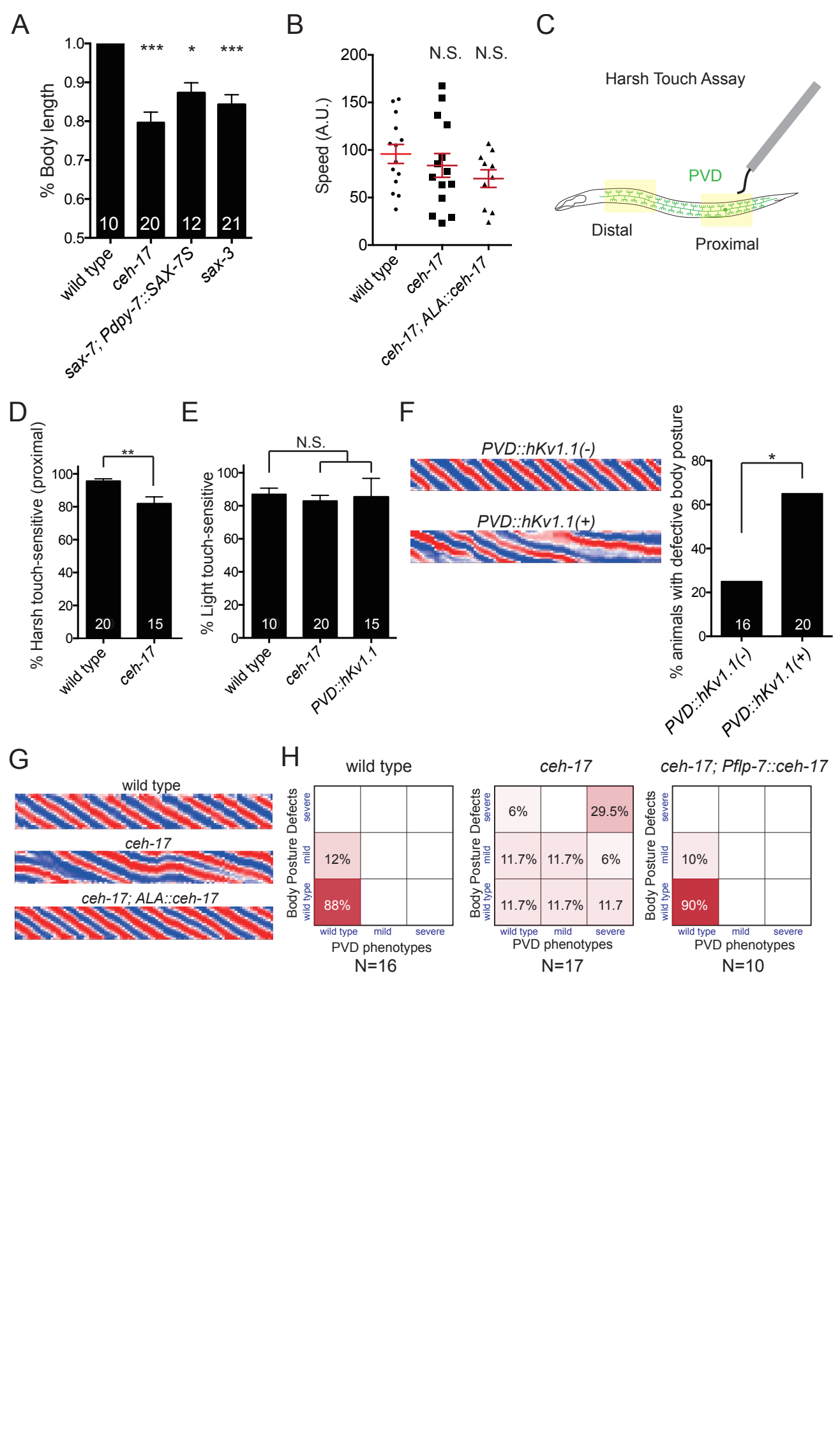
A
% Body length
1.0
0.9
0.8
0.7
0.6
0.5
***
*
***
10
20
12
21
wild type
ceh-17
sax-7; Pdpy-7::SAX-7S
sax-3
B
Speed (A.U.)
200
150
100
50
0
N.S.
N.S.
wild type
ceh-17
ceh-17; ALA::ceh-17
C
Harsh Touch Assay
PVD
Distal
Proximal
D
% Harsh touch-sensitive (proximal)
100
80
60
40
20
0
**
20
15
wild type
ceh-17
E
% Light touch-sensitive
100
80
60
40
20
0
N.S.
10
20
15
wild type
ceh-17
PVD::hKv1.1
F
PVD::hKv1.1(-)
PVD::hKv1.1(+)
% animals with defective body posture
80
60
40
20
0
*
16
20
PVD::hKv1.1(-)
PVD::hKv1.1(+)
G
wild type
ceh-17
ceh-17; ALA::ceh-17
H
wild type
Body Posture Defects
severe
mild
wild type
12%
88%
wild type
mild
severe
PVD phenotypes
N=16
ceh-17
6%
29.5%
11.7%
11.7%
6%
11.7%
11.7%
11.7
N=17
ceh-17; Pflp-7::ceh-17
10%
90%
N=10

**Figure S6. Evaluation of Sensory Functions in Mutants with Defective PVD Dendrite Morphology. Related to Figure 6.**

(A) Quantification of PVD dendritic arbor size expressed as the ratio of body length covered by peripheral PVD branches. *, $p < 0.05$, ***, $p < 0.005$, one-way ANOVA. (B) Quantification of locomotion speed. Error bars are S.E.M. N.S., not significant, one-way ANOVA. (C) Schematic diagram of harsh touch test by a metal wire placed in different body regions. (D) Quantification of harsh touch sensitivity in proximal region. N = numbers of animals scored. Error bars = S.E.M. **, $p < 0.01$, Student *t* test. (E) Quantification of light touch sensitivity. N = numbers of animals scored. Error bars = S.E.M. N.S., not significant, one-way ANOVA. (F) Quantification of body curvature defects with or without silencing PVD neural activity by hKv1.1. N = numbers of animals scored. *, $p < 0.05$, two-proportion z test. (G) Representative body curvature matrices for indicated genotypes. (H) Correlation of PVD morphology and body curvature pattern. N = animals scored.

**Movie S1. Movie of PVD growth cones in the wild type at L2 larval stage. Related to Figure 4.**

The growth cone is labeled by *twnEx398(Pser-2.3::GFP, Pflp-7::mCherry)*. The imaging covers a period of around 2 hours, with 8 minutes elapsed time between movie frames. Selective frames from this video were shown in Figure 4B.

**Movie S2. Movie of PVD growth cones in the *sax-7(nj48)* mutant at L2 larval stage. Related to Figure 4.**

The growth cone is labeled by *twnEx398(Pser-2.3::GFP, Pflp-7::mCherry)*. The imaging covers a period of around 3 hours and 30 minutes, with 14 minutes elapsed time between movie frames. Selective frames from this video were shown in Figure 4B.

**Movie S3. Movie of PVD growth cones in the *sax-3* mutant at L2 larva stage. Related to Figure 4.**

The growth cone is labeled by *twnEx398(Pser-2.3::GFP, Pflp-7::mCherry)*. The imaging covers a period of around 3 hours, with 8 minutes elapsed time between movie frames. Selective frames from this video were shown in Figure 4B.

**Movie S4. Movie of F-actin in the wild type at L2 larval stage. Related to Figure 5.**

F-actin is labeled by *twnEx400(Pser-2.3::LifeAct::NeonGreen)*. The imaging covers a period of around 20 minutes, with 2 minutes elapsed time between movie frames. Selective frames from this video were shown in Figure 5D.

**Movie S5. Movie of F-actin in the *ceh-17* mutant at L2 larval stage. Related to Figure 5.**

F-actin is labeled by *twnEx400(Pser-2.3::LifeAct::NeonGreen)*. The imaging covers a period of around 20 minutes, with 2 minutes elapsed time between movie frames. Selective frames from this video were shown in Figure 5D.

**Movie S6. Movie of F-actin in the *sax-7* mutant at L2 larval stage. Related to Figure 5.**

F-actin is labeled by *twnEx400(Pser-2.3::LifeAct::NeonGreen)*. The imaging covers a period of around 20 minutes, with 2 minutes elapsed time between movie frames. Selective frames from this video were shown in Figure 5D.